Donders Graduate School for Cognitive Neuroscience
Master of Science Programme
MSc Thesis

Changes in Resting-State Functional Connectivity in Patients with Neuralgic Amyotrophy

Melissa Bakkenes

Supervised by:

1. Ivan Toni, PhD.
2. Renee Lustenhouwer, MSc.

Radboud University Nijmegen

Date of final oral examination: 17-07-2020

Student name: Melissa Bakkenes

Student number: s1029912

Abstract

Neuralgic amoytrophy is a peripheral nervous system disorder, where the brachial plexus is affected. Neuralgic amyotrophy starts with an acute phase, which is likely caused by an acute auto-immune reaction against the brachial plexus. After the acute phase, patients with neuralgic amyotrophy often have motor problems, such as persisting abnormal posture and movement patterns of the scapula in the chronic phase. There are some indications that there could be a central nervous system problem, underlying the persisting long-term consequences of NA. Therefore, the aim of this project is to determine whether there is a difference in resting-state networks between neuralgic amyotrophy patients and healthy controls by comparing the brain activity of several resting-state brain networks between neuralgic amytrophy patients and healthy controls. To test this, we have performed a dual regression analysis with 41 neuralgic amyotrophy patients (mean age 43 ± 11 years, 16 females) with lateralized symptoms in the right upper extremity and 24 age and sex matched healthy controls (mean age 43 ± 8 years, 10 females). In addition, we assessed the specificity of a possible sensorimotor network resting-state fMRI difference in neuralgic amyotrophy patients compared to healthy controls, by considering the functional relevance of this difference on the motor impairments of NA patients. Furthermore, we wanted to evaluate if there are structural changes in the brain of patients with NA compared to healthy controls. In addition, we also wanted to evaluate whether possible resting-state fMRI changes in neuralgic amyotrophy patients are (partially) explained by structural changes in the brain. For these questions, a voxel based morphometry analysis was conducted. We have found that there is a difference in connectivity in the sensorimotor network and left frontoparietal network for neuralgic amyotrophy patients compared to healthy controls. There is no significant correlation between the sensorimotor network and capability of the upper-limb in neuralgic amyotrophy patients. There are also no significant group differences in grey matter volume. This study concludes

that a short inflammation of the brachial plexus can lead to task-independent functional reorganization of the central nervous system in patients with neuralgic amyotrophy. This finding could aid in the treatment for the persisting motor deficits in patients with neuralgic amyotrophy.

Keywords: neuralgic amyotrophy, upper extremity, peripheral nervous system disorder, maladaptive neuroplasticity, functional connectivity and grey matter volume

Changes in Resting-State Functional Connectivity in Neuralgic Amyotrophy

A core feature of the brain is its capacity to adapt in response to external stimuli, in other words, to change under physiological conditions, such that it contributes to memory, learning and brain development. The brain can functionally recover from acute or chronic brain injuries because of its neural plasticity mechanisms (Zeller & Classen, 2014). This functional recovery can happen due to compensatory mechanisms. Consequently, if one circuit fails then another circuit can take over and prevent deficits in the behavior (Helmich, de Lange, Bloem, & Toni, 2007). There are several central nervous system disorders where this phenomenon is seen, one example of such a disorder is a stroke. There is clinical evidence that the intact hemisphere plays an important role for the compensation of the damaged hemisphere, such that there is an optimal functional recovery after a stroke (Hara, 2015).

However, the brain's plasticity can also be maladaptive, which means that the neural plasticity in the brain leads to a disruption of the function (X. Y. Li et al., 2016). This means that mechanism cannot compensate for this disruption and adjusting the circuit can lead to modifications that are maladaptive. This maladaptive plasticity can, for example, be a compensatory movement pattern in patients with a stroke (Jang, 2013). Maladaptive plasticity is not only seen in central nervous system disorders, but also in several peripheral nervous system disorders (PNS), such as brachial plexus injury (BPI) (Bhat, Indira Devi, Bharti, & Panda, 2017; Feng et al., 2016) and carpal tunnel syndrome (CTS) (Maeda et al., 2014). BPI is a traumatic peripheral nerve injury of the brachial plexus which leads to sensory and motor losses of the affected limb (Bhat et al., 2017; Liu et al., 2013; Lou, Shou, Li, Li, & Gu, 2006; Reddy et al., 2002). CTS is a peripheral nerve injury where the median nerve is entrapped (Maeda et al., 2014). It is known that these peripheral nerve injuries lead to functional and structural changes in the brain. For example, there is an altered functional connectivity within

the sensorimotor network (SMN), frontoparietal network (FPN), salience network (SN), default mode network (DMN) and executive control network (ECN) in patients with BPI compared to healthy controls (Bhat et al., 2017; Feng et al., 2016). In addition, there is maladaptive neuroplasticity in the somatosensory cortex in patients with CTS (Maeda et al., 2014). Furthermore, there is a decrease in grey matter volumes of the cerebellum, anterior cingulate cortex (ACC), and bilateral frontal lobe in patients with BPI compared to healthy controls (Lu et al., 2016). Another PNS in which central changes may occur, is Neuralgic Amyotrophy (NA). Similarly to BPI, the nerves in the brachial plexus are damaged in NA. NA is therefore comparable with BPI regarding the central changes. However, it is unknown if the peripheral changes in NA lead to functional cortical reorganization. Therefore, the aim of this project is to understand and determine whether there are functional and structural changes in the central nervous system in patients with NA.

The exact cause of NA is unknown, but NA starts with an “attack” in the acute phase, which is likely caused by an acute auto-immune reaction of the brachial plexus. Patients with NA have extreme pain at onset, multifocal paresis and atrophy of upper limb muscles in the acute phase (Van Eijk, Groothuis, & Van Alfen, 2016). In 70 % of the NA patients, the long thoracic nerve, which innervates the serratus anterior muscle, is affected. This muscle is weakened in the acute phase and leads to compensatory, abnormal positioning and movements of scapula in the chronic phase, which affects the functional capability of the upper extremity (Cup et al., 2013). A way to assess functional capability of the upper extremity is with the Disability of the Arm, Hand and Shoulder (DASH) questionnaire (Gummesson, 2003). It is known that the DASH correlates with functional changes in the brain in PNS disorders (Feng et al., 2016; Gummesson, 2003). However, it is unknown if there is a relation between the functional capability and the possible changes of the functional reorganization in the brain of patients with NA.

Recovery of NA is usually slow and only 10% of the patients does fully recover (Van Eijk et al., 2016). Patients with NA often still have motor problems, such as persisting abnormal posture and movement patterns of the scapula in the chronic phase, also known as scapular dyskinesia (Cup et al., 2013; Van Eijk et al., 2016). There are some indications that there could be a central nervous system problem, underlying the persisting long-term consequences of NA. Firstly, the damaged nerves in the acute phase will recover over time and the strength of the affected muscles can return, as well as the stabilization of the serratus anterior muscle. However, the function of the shoulder often does not recover fully in the chronic phase. This indicates that peripheral nerve damage may lead to central adaptations, such as changes in motor planning and representations. Secondly, patients with NA have difficulty with the execution of functionally relevant trained movements of the shoulder coordination (Van Eijk et al., 2016). However, the NA patients do not have this difficulty with the execution of newly learned movements. Thirdly, the fatigability of the affected muscles does not fully recover. Patients with NA cannot change their activation pattern between fatigued and rested motor units during sustained contractions, as they could before the NA attack, which leads to peripheral fatigue. The incapability to alternate activation patterns of motor units, could indicate that central activation failure may also play a role in the residual complaints in the chronic phase of the NA patients (Van Eijk et al., 2016). Fourthly, a clinical pilot study of Ijspeert et al. (2013) had a specific outpatient multidisciplinary rehabilitation program focusing on regaining motor control, which normalizes scapular coordination and stability and improves functional capability of the upper extremity. This indicates that this specific rehabilitation program can improve the function of the shoulder, possibly by restoring the initial central adaptations, however this is still unknown. Fifthly, the study of Lustenhouwer et al. (2020) has investigated the central sensorimotor representations in patients with NA with a hand laterality judgement task (HLJT). In this task, subjects are

presented with pictures of hand, where the subjects should indicate the laterality (left or right) of the hand by using motor imagery. Lustenhouwer et al. (2020) has found that patients with NA showed an increased error rate for recognizing their affected right limb. This was not the case for healthy controls. This indicates that cerebral (mal)adaptations could play a role in motor dysfunction in NA, which is visible in the impaired performance in the HLJT.

Overall, the available evidence suggests that maladaptive motor planning could play a role in long-term symptoms and disability in NA. Relearning motor control can normalize scapular movements and stability by recruiting compensatory brain circuits, however there is no direct evidence for adaptive cerebral neuroplasticity in NA (W. Li, Li, Zhu, & Chen, 2014; van Nuenen et al., 2012; Zeller & Classen, 2014). A way to investigate these central mechanisms is through resting-state functional magnetic resonance imaging (rs-fMRI) (Beckmann, DeLuca, Devlin, & Smith, 2005). This neuroimaging technique measures changes in blood oxygen level dependent (BOLD) signal across time in resting states (Lee, Smyser, & Shimony, 2013). When these signal variations are temporally correlated across the brain, they correspond to a resting-state network (Beckmann et al., 2005). It should be noted that, resting-state networks have a functional hierarchy and this same functional hierarchy is seen during a task. This indicates that task-evoked activity can be predicted from resting-state data and aid in finding the underlying explanation for differences in brain activity induced by an experimental task (Travor et al., 2016). Differences in brain activity between groups induced by an experimental task can be the consequence of subject using different strategies that involve different brain circuits (Travor et al., 2016). Furthermore, abnormalities in resting-state networks are related to pathological conditions, therefore rs-fMRI offers a noninvasive way to look at functional network structures (Greicius et al., 2007). A better understanding of the central plasticity after peripheral nerve injuries can help by giving

insight into consequences of NA and may help in improving the long-term symptoms in patients with NA.

Therefore, the aim of this project is to determine whether there is a difference in resting-state networks between NA patients and healthy controls by comparing the brain activity of resting-state brain networks between NA patients and healthy controls. This is the first study that investigates the functional and structural brain changes in patients with NA, hence little is known about the cerebral changes in NA. Consequently, the hypotheses of the research questions will mainly be based on the findings of BPI. As mentioned before, BPI is a peripheral nervous disorder which is characterized by a traumatic injury of the brachial plexus, which has cerebral changes as a consequence (Bhat et al., 2017; Feng et al., 2016; Lu et al., 2016). The same plexus is affected as in NA, hence BPI is a reasonable proxy for NA. However, NA is characterized by an auto-immune inflammation of the brachial plexus and therefore not traumatic (Van Eijk et al., 2016). It is known from the literature that there is less resting-state functional connectivity in the sensorimotor network (SMN) in BPI patients compared to healthy controls, because there is a loss of motor and sensory functions in these patients (Bhat et al., 2017; Feng et al., 2016). In this project, the patients with NA have sensory and motor losses of their upper extremity. Therefore, it is expected that the patients with NA have an altered SMN connectivity compared to healthy controls. Furthermore, the execution and learning of movements engages the prefrontal and parietal cortex, which are regions involved in the FPN (Lam et al., 2018). The FPN is also a network involved and changed in patients with BPI (Feng et al., 2016). Therefore, it is expected that the patients with NA have an altered FPN connectivity compared to healthy controls, because they execute movements differently (Lam et al., 2018).

In addition, we assessed the specificity of a possible SMN rs-fMRI difference in NA patients compared to healthy controls, by considering the functional relevance of this

difference on the motor impairments of NA patients. We assessed this by looking at whether the potential difference in the SMN in patients with NA will correlate with the functional capability of the upper limb. Since the sensory and motor losses of the affected upper-limb are mediated by the SMN, it is expected that there is a correlation between the SMN and the functional capability of the upper-limb.

It is unknown if there is a structural reorganization in patients with NA, therefore we want to evaluate if there are structural changes in the brain of patients with NA compared to healthy controls. Furthermore, we also want to evaluate whether possible rs-fMRI changes in NA patients are (partially) explained by structural changes in the brain. For these questions, a voxel based morphometry analysis (VBM) will be conducted to see if there are changes in the cortical grey matter in patients with NA. Inferred from the findings of Maeda et al. (2014) and Lu et al. (2016), it is expected that patients with NA who are right side affected, will have a decrease in grey matter volumes of the left postcentral gyrus, bilateral frontal lobe, right cerebellum and the ACC compared to healthy controls.

Methods

Recruitment of subjects

This current study is part of a bigger study where the aim is to investigate the effect of NA on central motor representations, and the effect of a rehabilitation program (Ijspeert et al., 2013) on central changes. In this study, all patients participated in two or three measurement sessions, depending on the intervention group, with four months between each session. All sessions took place at the Donders Centre for Cognitive Neuroimaging and the Radboudumc in Nijmegen. A measurement session started with a MRI scan, where the subjects had three scans: a functional scan while performing a motor imagery task, a structural scan and a resting-state scan. Additionally, several other measurements were assessed: strength measurements, NENS task, measure of reachable workspace, questionnaires and a 3D-photo

of the shoulder in the RadboudUMC. Every session followed this exact order and had the same procedure, except for the first session. In this session, the NA patients were randomised into the rehabilitation or usual-care group. Patients in the rehabilitation group participated immediately in the rehabilitation program and the patients in the usual-care group needed to wait for four months to participate in the rehabilitation program. In this study we only focus on the rs-fMRI data of the first session of the NA patients. The healthy controls were assessed in a single session at the Donders Centre for Cognitive Neuroimaging and the Radboudumc. Written informed consent was obtained from all subjects before participation. Forty-seven NA patients were recruited through the specialized out-patient clinic at the RadboudUMC in Nijmegen. Six NA patients were excluded from this study, where two patients had NA bilaterally, one patient had a stroke, and the other three patients were not MRI compatible. Twenty-five age and sex matched healthy controls were recruited for cross-sectional comparison. One healthy control was excluded because of a history of shoulder problems. All patients and healthy controls were ≥ 18 years old, right-handed according to the Edinburgh Handedness Inventory (EHI) (score > 40)(Oldfield, 1971) and not suffering from depression (Beck Depression Inventory Fast Screen (BDI-FS) score ≤ 5)(Neitzer, Sun, Doss, Moran, & Schiller, 2012). The NA patients had lateralized symptoms in the right upper extremity and had scapular dyskinesia on the right side. NA patients in the acute phase (< 8 weeks since attack onset) were excluded. Also, the NA patients and healthy controls were MRI compatible and did not have any other neurological disorders or complaints of the upper extremity, other than NA. The research protocol was approved by the local medical-ethical committee (Medical Ethical Committee region Arnhem-Nijmegen, CMO 2017-3740). Between group difference in age was compared by performing an independent-samples *t*-test and between group difference in sex was compared using a Mann-Whitney U-test. Statistical analysis were performed using IBM SPSS Statistics (Corp, Released 2015). Statistical significance was

assumed when $p < .05$. Sample size was not powered on rs-fMRI effects, it was calculated based on the pilot study mentioned before from Ijspeert et al. (2013), with an effect size of 0.29, a power of 0.90 and two-tailed testing ($\alpha = 0.05$).

Imaging protocol

Imaging data was acquired through one MRI session. During the resting-state scan, the subjects were verbally instructed to lay still, to look at the cross in the center of the screen and to not think of anything in particular. This scan took about 7 minutes. For the structural (T1) scan, subjects were verbally instructed to lay still and to close their eyes. This scan took about 5 minutes. Head movement was minimized by using a memory foam around the subjects' head and by giving tactile feedback by spanning tape over the forehead that connects to both sides of the head coil. The resting-state functional images and anatomical images were acquired with a 3-Tesla Magnetom PrismaFit MR scanner from Siemens. For details of the scan parameters see table 1.

Table 1

Scan parameters for structural and resting-state MRI

Scan	Sequence	TR/TE/TI (ms)	Flip angle	FOV	Slices	Voxel-size (mm)	Scanning time (min)
T1	MPRAGE	2300/3.03/1100	8	256	192	1.0x1.0 x1.2	5.21
Rs-fMRI	Multiband 8	735/39/NA	52	210	64	2.4x2.4 x2.4	7

Note. The table consists of the scan parameters for the structural scan and the resting-state fMRI scan. T1 is the structural scan and rs-fMRI is the resting-state fMRI scan. Abbreviations: TR, repetition time, TE, echo time, TI, inversion time, FOV, field of view.

Preprocessing of Functional MRI images

The rs-fMRI data preprocessing was carried out using FEAT (FMRI Expert Analysis Tool) Version 6.00, part of FSL (FMRIB's Software Library, www.fmrib.ox.ac.uk/fsl). The

preprocessing steps included non-brain tissue extraction using the brain extraction tool (BET), motion correction using MCFLIRT and 3.6-mm full width at half-maximum (FWHM) spatial smoothing with a Gaussian kernel (Mark Jenkinson, Bannister, Brady, & Smith, 2002a, 2002b; S. M. Smith, 2002). Registration of the functional image to the high resolution structural image in Montreal Neurological Institute 152 (MNI 152) was carried out using FLIRT (Mark Jenkinson et al., 2002a, 2002b) Registration from high resolution structural to standard space was then further refined using FNIRT nonlinear registration (Andersson, Jenkinson, & Smith, 2007a, 2007b). No subjects were excluded because of head motion. Additional to these first preprocessing steps, ICA-AROMA (Pruim et al., 2015) was performed to remove motion artifacts, as well as non-motion noise components. Components were identified as motion or non-motion by ICA-AROMA, these were manually checked and reclassified if needed according to the article of Griffanti et al. (2017). This means that the components labeled as motion or non-motion were visually inspected on its spatial pattern, time series, and frequency spectrum. The components labeled as motion were removed. Furthermore, a nuisance regression was performed with two nuisance regressors: white matter (WM) and cerebrospinal fluid (CSF). These regressors were average time series of the WM and CSF masks created through tissue-type segmentation (Zhang, Brady, & Smith, 2001). Also, we have added 24 motion parameters, consisting of six primary realignment parameters, the history of the realignment parameters and the parameters squared to remove excessive head motion (Satterthwaite et al., 2013). In addition, we have also calculated the framewise displacement for every subject with a cut-off of 0.3 mm to assess the head motion between volumes. None of the subjects exceeded the 0.3 mm framewise displacement. Furthermore, a high-pass temporal filter (>0.01 Hz) was used to remove low-frequency oscillations from the BOLD signal. Finally, the final smoothing was calculated by taking the first smoothing (3.6-

mm FWHM) of the preprocessing into account. Therefore, the images were being smoothed with 4.8-mm FWHM Gaussian kernel for a final smoothing of 6.0-mm FWHM.

Data Analysis of the Resting-State fMRI

After preprocessing of the data, a multivariate group probability independent component analysis (ICA) was performed to get spatially independent components (Anderson, Goldstein, Kydd, & Russell, 2015). Due to unequal group sizes (NA patients = 41, healthy controls = 24), we needed to perform a temporal concatenation group ICA (TC-GICA), such that the unequal group size does not bias our data. By running Melodic multiple times with a different combination of 24 NA patients every time, this bias would be minimized. Subsequently, we did this by randomly picking 24 NA patients 500 times and running Melodic 500 times with the randomly picked NA patients combined with the 24 healthy controls. We have set the limit of Melodic to 20 components. Consequently, the output was 500 runs times 20 components, which resulted in 10000 components. These 10000 components were concatenated into a 4D file and this 4D file was ran again in Melodic and eventually the output consisted of the average 20 components of the 500 runs. For a schematic overview, see figure 1.

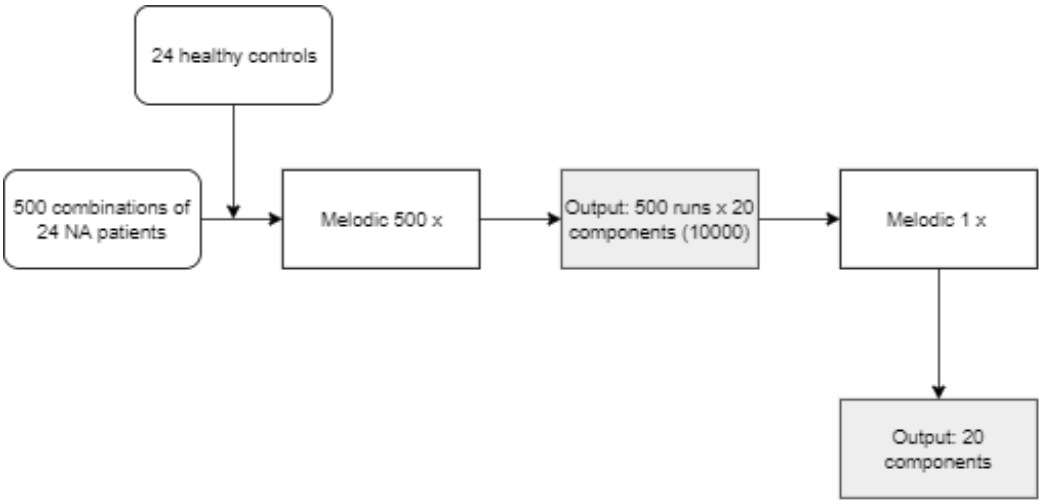

Figure 1. A flowchart of the TC-GICA, where we performed Melodic 500 times with 500 different combinations of 24 NA patients combined with 24 healthy controls. The output of those 500 runs from Melodic were used as input for the last Melodic. We have set the limit of Melodic to 20 components.

Out of the 20 components from Melodic, we have selected the components that corresponded with our network of interests, which are the SMN and FPN, based on visual inspection. In total, there were two components that corresponded with the left FPN, three components with the right FPN and three components with the SMN. We have also performed a correlation test to evaluate spatial correlations between the group-level ICA maps and the resting-state maps of Brainmap from S. M. Smith et al. (2009) and to see if this confirmed our visual inspection. This spatial correlation was calculated using the "fslcc" command of FSL (M. Jenkinson, Beckmann, Behrens, Woolrich, & Smith, 2012). The networks with a correlation greater than $r>0.3$ were considered for further analysis (Poudel et al., 2014). We selected one component for each network of interest, such that we eventually have three components for further analysis.

Next, dual regression analyses were performed for group wise comparisons of the independent components (Nickerson, Smith, Ongur, & Beckmann, 2017). In the first stage of the dual regression, we used our own group templates as the spatial regressors to get the subject specific time courses. These time courses were used as input in stage 2 to get subject specific spatial maps. Variance normalization was used to get the activity as well as the

spatial spread of the resting-state networks. The output of dual regression was tested voxel-wise for statistically significant differences between groups by using 5000 permutations with nonparametric permutation testing and corrected for Family-Wise Error by using a threshold free cluster enhancement technique (TFCE) to control for multiple comparisons (Winkler, Ridgway, Webster, Smith, & Nichols, 2014).

Group means of the components that correspond with the SMN and left FPN were transformed from t-values to z-values for both groups separately. This transformation was done with the function 'ttoz' in FSL (M. Jenkinson et al., 2012).

To evaluate if the significant clusters from the dual regression analysis were part of other resting-state networks components from the group template, than the resting-state network where the significant difference was found, we have created masks for all the significant clusters with by using the "fslstats" command of FSL (M. Jenkinson et al., 2012). Furthermore, we have masked all the components of our own group template with the mask of all the significant clusters to get the z-value for every cluster in every component.

Sensorimotor Network of NA patients and Capability of the Upper-limb

The capability of the upper extremity in NA patients was assessed with the Disability of Arm, Shoulder and Hand (DASH) questionnaire. The DASH is a self-administered questionnaire that assesses the capability of the arm, hand and shoulder and consists of a 30-item disability/symptom scale. Scores range from zero to hundred, where zero is no disability at all (Gummesson, 2003). This clinical outcome covers the activities and function domain of the International Classification of Functioning, Disability and Health (WHO, 2001).

To determine whether there is a correlation between the SMN and the capability of the upper-limb in NA patients, we used the z-maps per NA patient from output stage 2 of the dual regression. The z-maps per patient were split into separate components by using 'fslsplit' in

FSL (M. Jenkinson et al., 2012). The component that corresponded with the SMN was used for further analysis. The mean connectivity of the SMN component per subject was calculated by using 'fslstats' in FSL (M. Jenkinson et al., 2012). The correlation between the SMN and the DASH was calculated with a Spearman correlation using IBM SPSS Statistics(Corp, Released 2015). Statistical significance was assumed when $p < .05$. A Spearman correlation was used, because the mean connectivity of the SMN violated the auxiliary assumptions of normality.

Structural Analysis

Structural data were analyzed with FSL-VBM, which stands for voxel-based morphometry analysis carried out with FSL (Douaud et al., 2007; S. M. Smith et al., 2004). Due to unequal group size (NA patients = 41 and healthy controls = 24) we randomly selected 24 NA patients that were used for creating the grey matter (GM) template. The brain extracted subject T1 images, were needed for the tissue type segmentation, which was carried out per subject using FAST4 (Zhang et al., 2001). Then the study-specific GM template was created by registering all subject specific GM segmentations to standard space and averaging them. Registration to the study-specific template was done for all subjects and modulated by the warp field expansion (Jacobian) (Good et al., 2001) before being combined with non-linear registration across subjects into a 4D image. The modulated segmented images were then smoothed with a Gaussian kernel of 7.2-mm FWHM. Furthermore, voxel-wise GLM was applied using randomize from FSL. This function corrects for multiple comparisons across space with $p<0.05$ threshold by permutation based non-parametric testing with 5000 permutations (Winkler et al., 2014).

Results

Population characteristics

During the data analysis, no subjects were excluded. Table 2 shows an overview of the subjects' characteristics. All subjects were between 18 and 76 years old. There was no significant difference in age between the NA patients (M=43 years, SD=11 years) and healthy controls (M=43 years, SD=8 years), $t(63) = 0.067$, $p = 0.947$. There was also no significant difference in the proportion of males and females between the NA patients and healthy controls (U=479.0, p=0.835).

Table 2

Subjects' Characteristics

	NA patients (N=41)	Healthy Controls (N=24)	*p*-value
Age			0.947
Mean ± SD	43 ± 11	43 ± 8	
Min-Max	18 – 76	26-57	
Sex			0.835
Male	25 (61%)	14 (58%)	
Female	16 (39%)	10 (42%)	
DASH			
Mean ± SD	38.7 ± 18.5	N/A	
Min-Max	5.8 – 85.8	N/A	
Time Since Attack (Months)			
Mean ± SD	16.7 ± 32.0	N/A	
Min-Max	2.0 – 204.0	N/A	

Note. Statistical tests for age were performed with an independent samples t-test. Statistical tests for sex were performed with a Mann-Whitney U-test, since sex did not follow a normal distribution. There is no significant difference in age and sex between the NA patients and healthy controls.

Group differences in networks of interest

We analyzed if there was a difference in activity of the SMN and the FPN between NA patients and healthy controls. The major regions involved in the SMN are: post-central gyrus, pre-central gyrus and right putamen. The major regions involved in the FPN are: the

left middle frontal gyrus, left lateral occipital cortex, left inferior temporal gyrus, right crus II. Twenty independent components were identified in the full sample. We found differences in two components: the SMN component and left FPN component (Fig. 2).

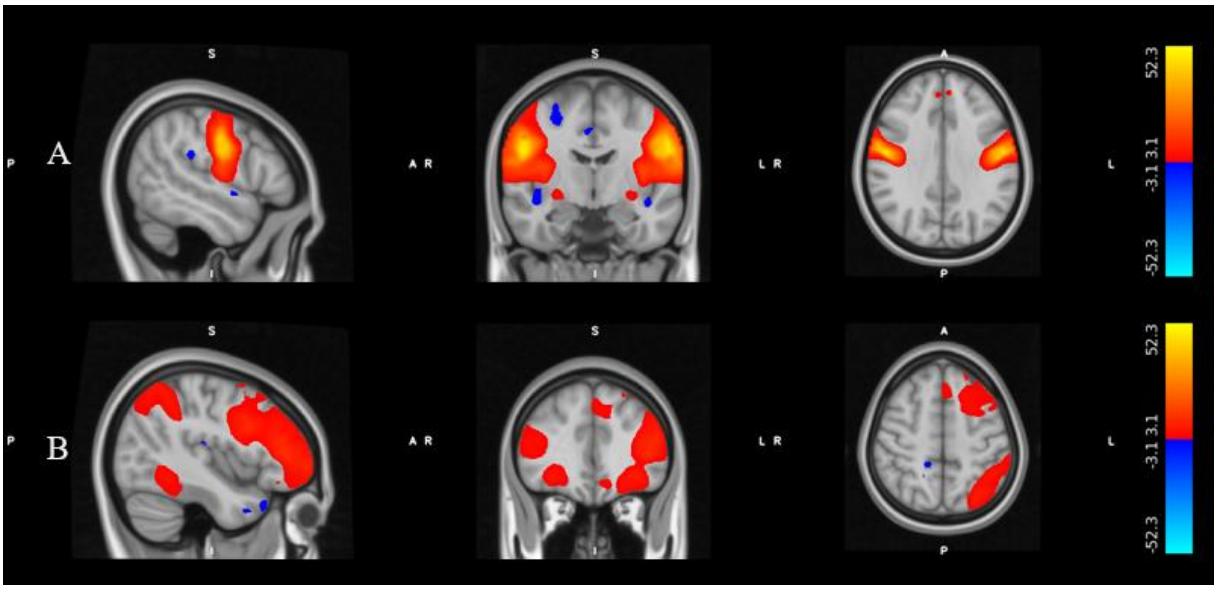

Figure 2: Independent components(IC) of the resting state networks identified in the full sample from Melodic. Sagittal, coronal and axial views of the spatial maps of our networks of interest: the SMN and the left FPN. The SMN consists of the postcentral gyrus, precentral gyrus, right putamen. The left FPN consists of the left middle frontal gyrus, left lateral occipital cortex, left inferior temporal gyrus, right crus II. The blue, red bar indicates minimum and maximum z-value of the SMN for the healthy controls and the NA patients. The images are shown with a statistical threshold of $z > 3.1$.

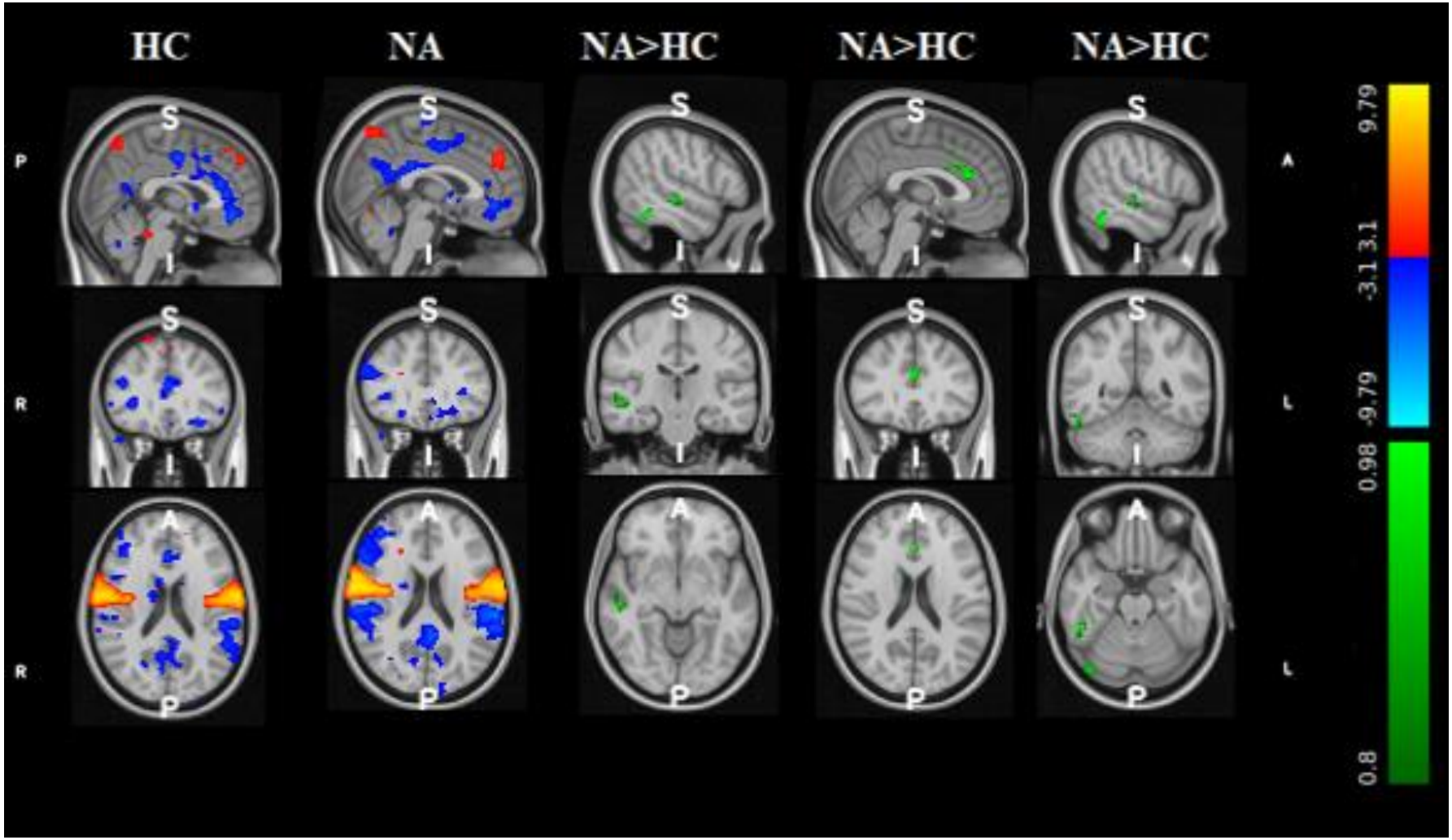

Figure 3: Functional MRI images of the SMN in healthy controls, NA patients and NA patients versus healthy controls shown in three planes: sagittal, coronal and axial. The first column contains the functional MRI images of the SMN for the healthy controls. The second column contains functional MRI images of the SMN for the NA patients. The third till fifth column contain the functional MRI images of the significant clusters in green, where the third column is the right inferior temporal gyrus (temporo-occipital part) (MNI coordinates peak-voxel: 48; -42; -24),, the fourth column is the right cingulate gyrus (anterior division) (MNI coordinates peak-voxel: 2; 30; 20) and the fifth column is the right middle temporal gyrus (posterior division) (MNI

coordinates peak-voxel: 54; -22; -8). The NA patients showed greater functional connectivity between the three clusters and the SMN than healthy controls). P = posterior, A = anterior, S = superior, L = left, R = right. The green bar indicates the minimum and maximum p-value of the significant clusters. Effects are shown at uncorrected p<0.20 for visualization purpose. The blue, red bar indicates minimum and maximum z-value of the SMN for the healthy controls and the NA patients. Images are shown with a statistical threshold of z > 3.1.

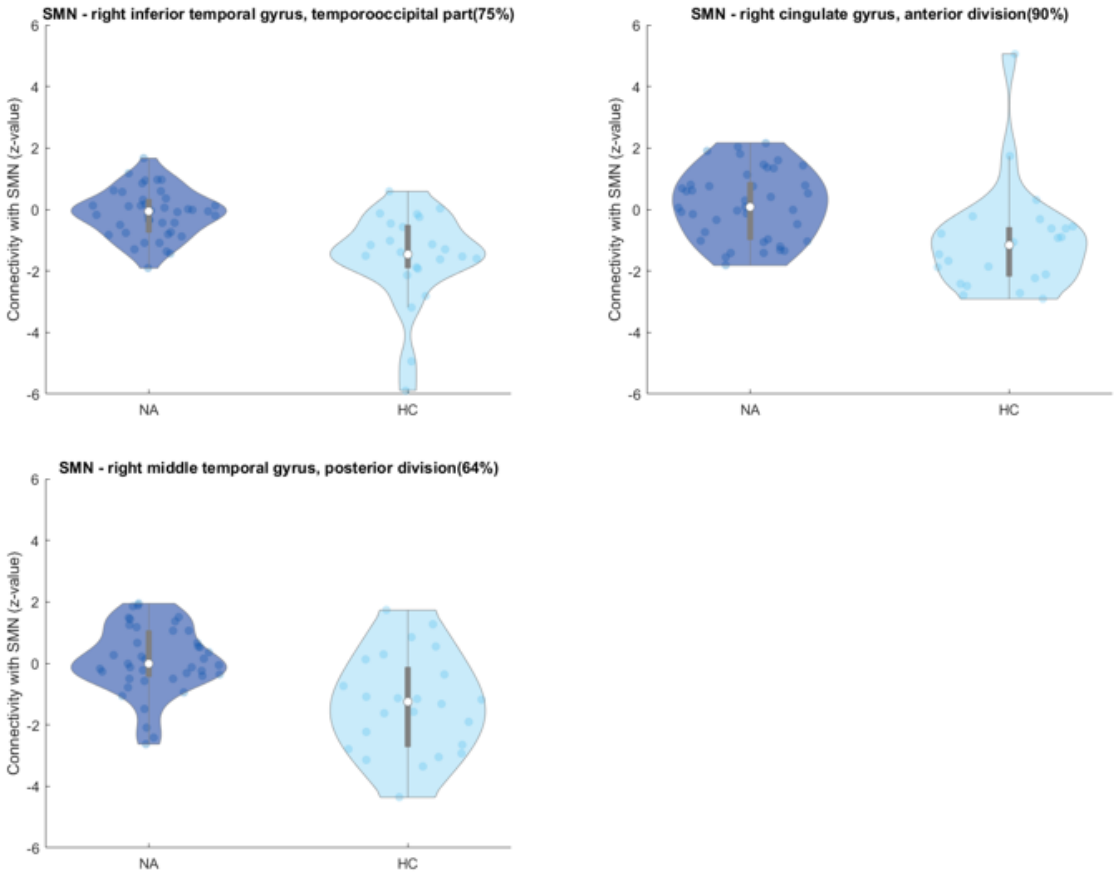

Figure 4: Violin plots show the median and the probability density of the connectivity value (Z-value) from the dual regression of the three significant clusters with the SMN for NA patients and healthy controls. The median Z-value of every cluster with the SMN is zero for the NA patients and negative for the healthy controls.

Sensorimotor Network

For the SMN, we found a group difference between the NA patients and healthy controls. Subsequently, there was a greater functional connectivity in three significant clusters with the SMN in NA patients compared to healthy controls. The three significant clusters were located in the right inferior temporal gyrus (temporo-occipital part) (MNI coordinates peak-voxel: 56; -50; -22, p-value = .02), the right cingulate gyrus (anterior division) (MNI coordinates peak-voxel: 2; 30; 20, p-value = .029) and the right middle temporal gyrus (posterior division) (MNI coordinates peak-voxel: 54; -22; -8, p-value = .047) for the SMN component (Fig.3; Fig 4; Table 4). Consequently, these three cluster have a different

connectivity with the SMN. As shown in figure 4, the right inferior temporal gyrus (temporo-occipital part), the right cingulate gyrus (anterior division) and the right middle temporal gyrus (posterior division) have a mean Z-value around zero for the NA patients, where this mean Z-value is negative for the healthy controls. This indicates that the NA patients have little or no correlation of the three clusters with the SMN and that the healthy controls have an anti-correlation of these clusters with the SMN.

Table 3

Mean connectivity value of the significant clusters from the SMN with left FPN component

	Brain regions		
	Right inferior temporal gyrus (temporo-occipital part)	Right cingulate gyrus (anterior division)	Right middle temporal gyrus (posterior division)
Left FPN (IC 11)	3.38	-2.84	-2.56

Mean z-values of the significant clusters from the SMN, in the left FPN component of the group template.

Further analyses have shown that the three significant clusters from the SMN have a mean z-value in the left FPN component of the group template, as shown in table 3. This means that the three significant clusters of the SMN are part of the left FPN component.

Table 4

Group mean effects on SMN images

Group	Brain regions	MNI Coordinates x	y	x	Cluster voxel	Peak z-stat
Healthy controls	Left precentral gyrus (47%)	-52	-8	32	4296	9.79
	Right postcentral gyrus (32%)	58	-6	22	3770	9.13
	Left precuneus (43%)	-6	-64	58	953	5.96
	Left cerebellum lobule VI (90%)	-16	-60	-22	501	8.25
	Right cerebellum lobule VI (85%)	16	-60	-20	468	7.87
	Right superior frontal gyrus (16%)	8	36	48	284	4.7

Group	Brain regions	MNI Coordinates x	y	x	Cluster voxel	Peak z-stat
	Right cerebellum lobule VIIIa (45%)	12	-64	-46	140	5.54
	Brain stem (84%)	-8	-38	-44	110	4.93
	Left superior frontal gyrus (60%)	-4	46	32	107	4.12
	Left cerebellum lobule VIIIa (50%)	-10	-64	-48	89	6.34
	Left angular gyrus (13%)	-62	-54	38	64	3.98
	Right thalamus (59%)	12	-18	-2	57	4.55
	Right superior frontal gyrus (48%)	20	30	60	54	3.7
	Left cerebellum lobule I-IV (10%)	0	-40	-26	47	4.81
	Right putamen (72%)	28	-8	-6	42	4.54
	Left lateral occipital cortex, superior division (10%)	-24	-60	32	31	4.07
	Left superior frontal gyrus (32%)	-18	24	52	30	4.17
	Left crus I (83%)	-44	-64	-40	21	3.72
NA patients	Left precentral gyrus (41%)	-52	-6	32	4635	9.56
	Right postcentral gyrus (40%)	48	-12	32	4051	9.62
	Right cerebellum lobule VI (95%)	18	-62	-18	1226	8.7
	Left precuneus (54%)	-6	-66	56	597	5.62
	Right superior frontal gyrus (67%)	6	48	36	581	4.91
	Left lateral occipital cortex, superior division (62%)	-32	-82	36	343	4.71
	Right cerebellum lobule VIIIa (52%)	10	-66	-46	133	6.48
	Left cerebellum lobule VIIIa (50%)	-10	-64	-48	125	6.56
	Right putamen (57%)	28	-8	-8	114	6.43
	Left superior frontal gyrus (43%)	-22	18	58	88	4.51
	Left postcentral gyrus (43%)	-22	-32	60	84	4.86
	Right angular gyrus (48%)	58	-48	40	60	4.1
	Left putamen (85%)	-28	-8	-6	46	4.51
	Right precentral gyrus (37%)	20	-30	60	44	4.19
	Left crus I (70%)	-22	-80	-32	30	3.83
	Right frontal pole (71%)	18	46	46	28	3.77
	Right thalamus (82%)	14	-18	0	23	4.38
	Brain stem (99%)	-4	-42	-50	23	4.04
	Right lateral occipital cortex, superior division (81%)	42	-76	38	23	3.89
NA patients > Healthy controls	Right inferior temporal gyrus, temporo-occipital part (75%)	56	-50	-22	47	0.02

Group	Brain regions	MNI Coordinates x	y	x	Cluster voxel	Peak z-stat
	Right cingulate gyrus, anterior division (90%)	2	30	20	42	0.029
	Right middle temporal gyrus, posterior division (64%)	54	-22	-8	2	0.047

Note. Anatomical labels for the SMN derived from the Harvard-Oxford cortical and subcortical structural atlases (Desikan et al., 2006) for 3 groups: healthy controls, NA patients and NA patients versus healthy controls. Coordinates were extracted from MNI 152 space. MNI-coordinates refer to largest z-value of a cluster and for the contrast NA patients > healthy controls MNI coordinates refer to the p-value of a cluster.

Left Frontoparietal Network

For the left FPN, we found a group difference between the NA patients and healthy controls. Subsequently, there was a greater functional connectivity in one significant cluster with the left FPN in NA patients compared to healthy controls. The significant cluster of the left FPN was located in the right thalamus (MNI coordinates peak-voxel: 22; -28; 2, p-value = 0.037) (Fig. 5; Table 5). Consequently, this cluster has a different connectivity with the FPN. As shown in figure 5, the cluster of the FPN has a mean Z-value of around zero for the NA patients, where this mean Z-value is negative for the healthy controls. This indicates that the NA patients have little or no correlation of the right thalamus with the FPN, where the healthy controls have an anti-correlation of this cluster with the FPN.

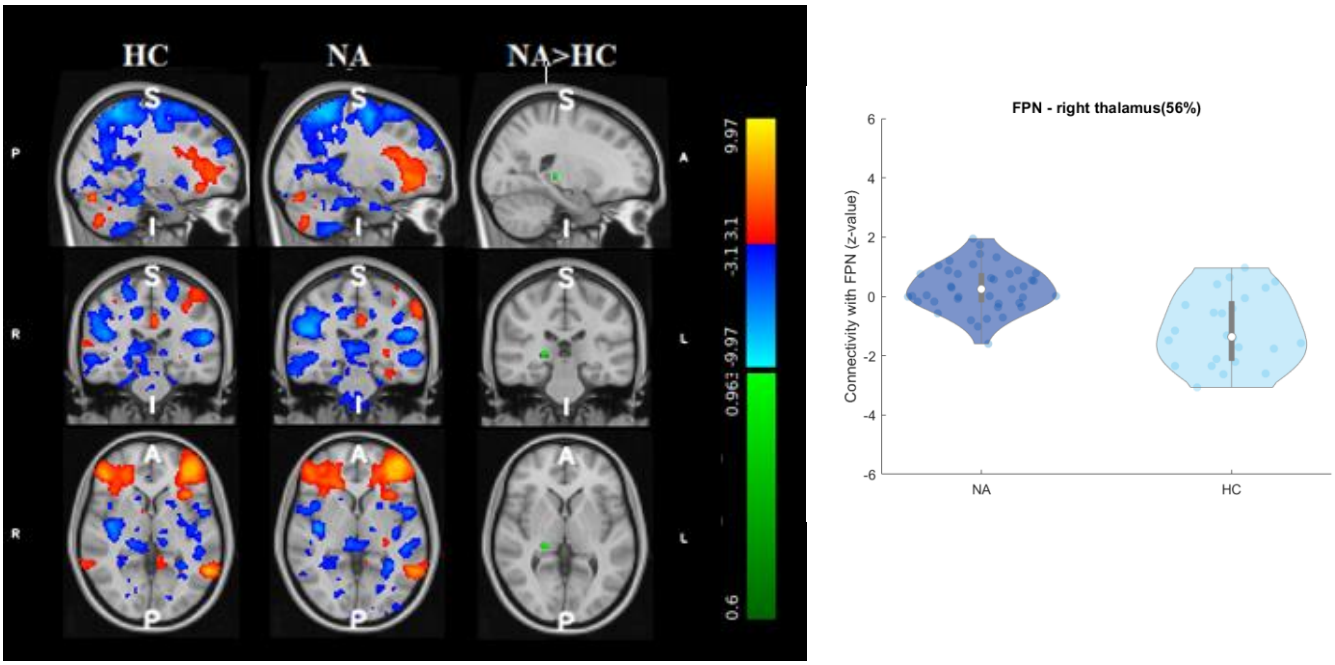

Figure 5: Functional MRI images of the FPN in healthy controls, NA patients and NA patients versus healthy controls. The NA patients showed greater functional connectivity between the significant cluster and the FPN than healthy controls. The significant cluster was located in right thalamus (MNI coordinates peak-voxel: 22; -28; 2). P = posterior, A = anterior, S = superior, L = left, R = right. Effects are shown at uncorrected p<0.40 for visualization purpose. Violin plot shows the median and the probability density of the connectivity value (Z-value) from the dual regression of the right thalamus with the FPN for NA patients and healthy controls. The median Z-value of this cluster is zero for the NA patients and negative for the healthy controls.

Table 5

Group mean effects on FPN images

Group	Brain regions	MNI Coordinates			Cluster voxel	Peak z-stat
		x	y	x		
Healthy controls	Left inferior frontal gyrus, pars triangularis (30%)	-42	30	20	24055	9.39
	Right crus I (47%)	12	-74	-28	2548	8.69
	Left middle temporal gyrus, temporo-occipital part (38%)	-54	-50	-8	2241	9.08
	Left cerebellum lobule VI (53%)	-10	-72	-28	1050	7.33
	Left precuneus (36%)	-6	-52	14	592	7.54
	Right middle temporal gyrus, temperooccipital part (67%)	60	-48	-2	407	5.26
	Left cingulate gyrus (60%)	-4	-32	34	400	7.14
	Left occipital pole (41%)	-14	-90	32	327	4.8
	Right supramarginal gyrus, posterior division (35%)	56	-38	14	274	5.01
	Left caudate (50%)	-16	-10	20	100	5.37
	Left cingulate gyrus, anterior division (30%)	-4	6	26	90	6.31
	Right caudate (52%)	10	6	6	90	4.7

Group	Brain regions	MNI Coordinates x	y	x	Cluster voxel	Peak z-stat
	Right lateral occipital cortex, superior division (69%)	34	-70	42	74	4.22
	Left hippocampus (82%)	-20	-12	-18	58	4.7
	Left crus I (100%)	-38	-68	-28	40	5.5
	Right occipital pole (37%)	14	-88	34	23	3.79
NA patients						
	Left frontal pole (43%)	-44	38	12	21627	9.76
	Left lateral occipital cortex, superior division (63%)	-30	-64	46	5625	9.97
	Right crus I (53%)	12	-74	-26	3878	9.9
	Left middle temporal gyrus, temporo-occipital part (34%)	-56	-52	-10	2796	9.01
	Right precentral gyrus (37%)	46	-14	56	656	5.66
	Left cingulate gyrus, posterior division (63%)	-4	-32	32	409	6.66
	Left precuneus (50%)	-6	-54	12	379	6.58
	Right inferior temporal gyrus, temporo-occipital part (68%)	54	-46	-14	199	5
	Left cingulate gyrus, anterior division (18%)	-4	4	26	157	6.79
	Left amygdala (96%)	-22	-4	-16	97	5.35
	Right cuneal cortex (72%)	2	-86	22	81	4.68
	Right occipital pole (44%)	12	-88	34	69	4.17
	Right caudate (78%)	12	-2	18	42	4.56
	Left superior temporal gyrus, posterior division (36%)	-66	-32	12	25	3.75
	Left caudate (63%)	-14	-10	20	23	4.82
	Left occipital pole (63%)	-4	-94	26	21	3.71
NA patients > Healthy controls						
	Right thalamus (56%)	22	-28	2	4	0.037

Note. Anatomical labels for the left FPN derived from the Harvard-Oxford cortical and subcortical structural atlases (Desikan et al., 2006) for 3 groups: healthy controls, NA patients and NA patients versus healthy controls. Coordinates were extracted from MNI 152 space. MNI-coordinates refer to largest z-value of a cluster and for the contrast NA patients > healthy controls MNI-coordinates refer to p-value of a cluster.

Sensorimotor Network of NA Patients and Capability of the Upper-limb

We have examined the relation between the SMN and the DASH, but there was no significant correlation between the SMN and the DASH, r(39)=.199, *p*= .212.

Structural Changes

Changes in The grey matter were assessed by a two-sample t-test comparing NA patients with healthy controls. The VBM analysis did not show any significant differences in grey matter volume between NA patients and healthy controls (Table 6).

Table 6

Voxel-based Morphometry Results

Group	Brain regions	MNI Coordinates x	y	x	Cluster voxel	p-value
Healthy Controls>NA Patients	Cingulate Gyrus, posterior division(6%)	-8	-32	30	58	0.63
NA Patients>Healthy Controls	Inferior Frontal Gyrus, pars opercularis (11%)	62	18	20	10	0.46

Note. Non-significant differences in grey matter volume between NA patients and healthy controls. Anatomical labels are derived from the Harvard-Oxford cortical and subcortical structural atlases (Desikan et al., 2006), Coordinates were extracted from MNI 152 space. MNI-coordinates refer to largest p value of a cluster.

Discussion

This study explored whether the alterations of the peripheral nervous system experienced by patients with NA lead to structural and connectivity changes in their central nervous system. We expected to see an altered functional connectivity in the SMN and left FPN for the NA patients compared to the healthy controls. Furthermore, we explored whether changes in SMN connectivity and structure had a relation to the clinical impairments of the patients, as indexed by functional capability of the upper-limb in NA patients. Our results confirm our hypothesis that there are resting-state network changes in patients with NA compared to healthy controls.

Group differences in networks of interest

In line with our hypothesis, we have found a significant difference in resting-state connectivity with the SMN and the left FPN networks in NA patients compared to healthy controls. This means that the connectivity of these significant clusters with the main regions of the resting-state network is different for NA patients compared to healthy controls.

Sensorimotor Network

The SMN is activated during motor tasks and involved in motor-planning, initiation, execution and coordination (Biswal, Yetkin, Haughton, & Hyde, 1995; Solodkin, Hlustik, Chen, & Small, 2004). As mentioned before, we have found a significant difference in the SMN for the NA patients compared to the healthy controls, which is consistent with the findings of the studies in BPI (Bhat et al., 2017; Feng et al., 2016). However, whereas these studies have found altered connectivity of a region within the SMN for the BPI patients, group differences in the current study were found in three regions outside the SMN: the right inferior temporal gyrus (temporal-occipital part), the right cingulate gyrus (anterior division) and the right middle temporal gyrus (posterior division). The NA patients have a connectivity score around zero of these clusters with the SMN component, where the healthy controls have a negative connectivity score, as shown in figure 4. This means that the NA patients have no correlation of these clusters with the SMN, whereas the healthy controls have an anti-correlation. The significant clusters of the SMN component are part of the left FPN component of our group template. This indicates that there is an altered connectivity between the SMN and the left FPN in NA patients compared to healthy controls. In line with our findings, studies in BPI have shown an altered connectivity of the FPN in patients with BPI compared to healthy controls (Bhat et al., 2017; Feng et al., 2016). Specifically, we have found a change in functional connectivity between the SMN and left FPN in NA patients compared to healthy controls. Feng et al. (2016) has looked at the connectivity between

resting-state networks in patients with BPI, however they have found a decreased connectivity between the SMN and the right FPN. Feng et al. (2016) has recruited BPI patients without any pain, to rule out the influence of pain. Our study does have NA patients that have experienced pain, this could indicate why we find different results compared to Feng et al. (2016). Functional connectivity between the SMN and the FPN is involved in conveying visual sensory inputs into movement planning, preparation and execution (Staines, Padilla, & Knight, 2002). Related to our findings, this could mean that the SMN gets reduced access to visual information and could indicate that the NA patients have an altered motor planning compared to healthy controls. This confirms the indications that there are cerebral changes in NA patients, which could contribute to the residual motor complaints in NA. Our findings do regard the resting-state fMRI and not the task-based fMRI. Consequently, it remains unknown whether the altered connectivity generalizes to a situation where the subjects are planning to move on the basis of visual information.

Left Frontoparietal Network

The left fronto-parietal regions of the FPN are involved in spatial working memory (Paulraj, Schendel, Curran, Dronkers, & Baldo, 2018). We have found a significant difference in the left FPN for the NA patients compared to the healthy controls, which is consistent with the findings of a study in BPI (Feng et al., 2016). However, whereas that study has found altered connectivity of a region within the left FPN, the group difference in the current study was found in a region outside of the left FPN: the right thalamus. This pattern is also seen in the SMN and could be an indication that the NA patients have more segregated resting-state networks than healthy controls. The specific area of the thalamus that is significant in the left FPN component, is the dorsal pulvinar (A. T. Smith, Cotton, Bruno, & Moutsiana, 2009). The NA patients have a connectivity score around zero of the right thalamus with the left FPN, where healthy controls have a negative connectivity score of this cluster with the left FPN.

Since the NA patients are right-side affected, consequently the motor areas of the left hemisphere are possible changed. These motor areas are involved in predicting and accounting for limb dynamics (Schaefer, Haaland, & Sainburg, 2009). This could explain our finding of altered connectivity with the left FPN, since the left FPN also has a connectivity with the SMN (Staines et al., 2002). There is not a clear explanation for why we have found a connectivity of the right thalamus with the left FPN. The left thalamus has a different connectivity with the left FPN than the right thalamus, the connectivity score of the left thalamus is positive for the NA patients as well as the healthy controls. This indicates that there is a lateralization of the thalamus. It is proposed that the right thalamus is specialized in non-verbal, spatial information (Gupta & Tranel, 2012). Since there is an indication that NA patients do have difficulty with motor planning, this could be an indication for why we have found a significant connectivity difference of the right thalamus with the left FPN for the NA patients compared to the healthy controls. The thalamus is known to integrate incoming sensory information and to influence multisensory processing of cortical regions, thereby playing an important role in motor and sensory relay functions (Peters, Dunlop, & Downar, 2016; Tyll, Budinger, & Noesselt, 2011). The thalamus has a regulatory role in brain networks and could be a hub of anti-correlation (Gopinath, Krishnamurthy, Cabanban, & Crosson, 2015). The shift between positive correlation and anti-correlation of the thalamus with cortical regions is a shift between alertness and rest. A decreased anti-correlation can indicate an impairment of this inhibitory aspect of the thalamus (Ramkiran, Sharma, & Rao, 2019). Grieve, Acuna, and Cudeiro (2000) suggests that the connectivity between the FPN and the dorsal pulvinar contributes to complex visuomotor transformations that requires integration of visual eye and hand position information. The study of Edwards, King, Buetefisch, and Borich (2019) states that to have an efficient motor plan, it is important to have successful integration of information. Related to our findings, this could mean that the

NA patients have less coupling between the right thalamus (dorsal pulvinar) and left FPN than the healthy controls, hence have less sensorimotor integration. This could indicate the altered motor planning in NA patients, which possible underlies the persisting motor deficits of the upper-limb.

Sensorimotor Network of NA Patients and Capability of the Upper-limb

We did not find a correlation between the SMN and the capability of the upper-limb. This negative finding raises doubts on the clinical relevance of the fMRI observations. To assess the capability of the upper-limb, we have used the DASH questionnaire. The DASH contains questions about the symptoms, pain, and restrictions in daily activities over a period of a week. NA is a heterogeneous disorder with phenotypic variability (Van Eijk et al., 2016), which is visible in the DASH score shown in table 2. The minimum DASH score is 5.8 and the maximum DASH score is 85.8. This indicates that the DASH score, and thereby the capability of the upper-limb, varied between the NA patients. In addition, the sample size of our study limits the statistical power, therefore it is possible that only large brain-behavior correlations could have been identified.

Structural Changes

Despite the functional changes in the brain, we did not find any structural brain differences between the NA patients and healthy controls, which is not in line with our hypothesis. Furthermore, this finding is not consistent with the findings from a study in BPI (Lu et al., 2016). There are several factors that could underlie the absence of the structural group difference between NA patients and healthy controls. Firstly, we have performed a whole brain analysis, which has less statistical power than a region of interest analysis. A whole brain analysis requires correction for multiple comparisons which decreases statistical power, whereas this is not needed for a region of interest analysis (Cremers, Wager, &

Yarkoni, 2017). This means that there is a higher probability of failing to reject the null hypothesis and could be a factor for not finding a significant group difference. Secondly, the time between the NA attack and the first measurement session was different between the NA patients, as shown in table 2. The minimum time between the NA attack and the measurement session is two months and the maximum time is seventeen years. This indicates that the time since the NA attack is variable between the NA patients, which could have played a role in not finding a significant structural group difference between NA patients and healthy controls. In addition, patients who had NA for several years could have different structural brain changes compared to patients who had NA for two months, because they could have applied different compensation strategies for the functional deficit that goes with the long-term symptoms of NA. Thirdly, the phenotypic variability in NA patients could also be a factor in not finding structural brain differences between NA patients and healthy controls. The location of the paresis differed between the NA patients, which could lead to different alterations of somatosensory input. Consequently, to different structural brain changes between the NA patients (Di Vita et al., 2018).

Clinical Relevance

In line with many other studies of peripheral nervous system disorders (Bhat et al., 2017; Feng et al., 2016; Maeda et al., 2014), our findings confirm that peripheral nerve damage leads to cerebral changes. More specifically, peripheral nerve damage in NA leads to cerebral changes and may underlie the long-term symptoms in NA. Despite the peripheral nerve recovery, there are still motor deficits and it is possible that the changes in resting-state networks could play a role. The SMN has an altered connectivity with the left FPN in NA. Furthermore, NA patients possibly have less sensorimotor integration due to reduced coupling between the right thalamus (dorsal pulvinar) and the left FPN. These findings could indicate altered motor planning that could contribute to the residual motor complaints in patients with

NA. Therefore, this finding may have important implications for the treatment of NA. The clinical pilot study of Ijspeert et al. (2013) focus on the changed movement patterns. The NA patients participating in the study of Ijspeert et al. (2013) do regain their motor function by focusing on regaining motor control. Our finding could be an indication that NA patients do have cerebral changes as a consequence of NA and that the rehabilitation program of Ijspeert et al. (2013) could possibly aid in changing resting-state networks and improving the long term symptoms in patients with NA. However, further research is needed to confirm our exploratory findings. For example, by investigating the effect of the rehabilitation program (Ijspeert et al., 2013) in NA patients by comparing resting-state functional connectivity before and after the specific rehabilitation program in NA patients.

Strengths and limitations

This study has several strengths and limitations. Firs, our study is the first study that has evaluated the resting-state network changes and structural changes of the brain in patients with NA and is part of a larger randomized controlled trial study investigating the effect of NA on central motor representations and the effect of specific rehabilitation. The findings of this study could help improve the treatment for the persisting motor deficits in patients with NA. Secondly, we compared NA patients to a well matched healthy control group, which means that any group differences are not due to age or sex. Thirdly, we have used rs-fMRI as a method to assess the functional changes of the brain. Task-evoked activity can be predicted from resting-state data and aid in finding the underlying explanation for differences in brain activity induced by an experimental task (Travor et al., 2016). Furthermore, abnormalities in resting-state networks are related to pathologic conditions, therefore rs-fMRI offers a noninvasive way to look at functional network structures (Greicius et al., 2007). Fourthly, it is important to note that we did not perform a global signal regression in the preprocessing pipeline of the rs-fMRI data, because using global signal regression can induce artifacts that

could give rise to anti-correlations between brain regions (Murphy, Birn, Handwerker, Jones, & Bandettini, 2009).

Despite its novel results, there are some limitations to this study. Firstly, having an unequal group size could have been a limitation for the VBM analysis. For the grey matter template, we have randomly chosen 24 out of 41 NA patients. Together with the heterogeneous phenotypic variability in NA patients, these could have played a role in not finding significant structural group differences. However, we did control for an unequal group size in our functional MRI data by creating a template, where we have used a temporal concatenation group ICA with multiple runs in Melodic. Secondly, NA is a heterogeneous disorder with phenotypic variability (Van Eijk et al., 2016). This heterogeneity was also apparent in our sample. Some patients with NA did not experience any pain, but had many motor problems, whereas others did not have any motor problems, but experienced a lot of pain. This phenotypic variability could also have an influence on the functional and structural MRI data analysis and could explain why we did not find any structural brain differences between NA patients and healthy controls and did not find a correlation between the capability of the upper-limb and the SMN in NA patients. A suggestion for further research would be to recruit more NA patients and perform subgroup analyses on these patients, which exclude some aspects of the heterogonous phenotypic variability. However, NA is often not recognized by a general practitioner (Van Eijk et al., 2016), which could make the recruiting of more NA patients difficult. Thirdly, we cannot make clear statements about the direction and strength of the correlation between the significant clusters and the resting-state networks, because we only performed a dual regression analysis. Further research is needed to make meaningful conclusions and interpretations about the connectivity between the significant clusters and the resting-state networks. For example, a study that only focusses on the FPN

and SMN connectivity changes in NA patients by using graph-theoretical analyses on network connectivity structure.

Conclusion

In summary, we examined the functional and structural changes throughout the brain in NA patients. Our results provided new evidence that there are changes in the SMN and left FPN network in patients with NA and that these changes could play a role in the persistent motor deficits in the chronic phase of NA. The findings of this study could aid in the treatment for the persisting motor deficits in patients with NA.

References

Anderson, V. M., Goldstein, M. E., Kydd, R. R., & Russell, B. R. (2015). Extensive gray matter volume reduction in treatment-resistant schizophrenia. *Int J Neuropsychopharmacol, 18*(7), pyv016. Retrieved from https://www.ncbi.nlm.nih.gov/pubmed/25716781. doi:10.1093/ijnp/pyv016

Andersson, J. L. R., Jenkinson, M., & Smith, S. M. (2007a). Non-linear optimisation. *FMRIB technical report*.

Andersson, J. L. R., Jenkinson, M., & Smith, S. M. (2007b). Non-linear registration, aka Spatial normalisation. *FMRIB technical report*.

Beckmann, C. F., DeLuca, M., Devlin, J. T., & Smith, S. M. (2005). Investigations into resting-state connectivity using independent component analysis. *Philos Trans R Soc Lond B Biol Sci, 360*(1457), 1001-1013. Retrieved from https://www.ncbi.nlm.nih.gov/pubmed/16087444. doi:10.1098/rstb.2005.1634

Bhat, D. I., Indira Devi, B., Bharti, K., & Panda, R. (2017). Cortical plasticity after brachial plexus injury and repair: a resting-state functional MRI study. *Neurosurg Focus, 42*(3), E14. Retrieved from https://www.ncbi.nlm.nih.gov/pubmed/28245732. doi:10.3171/2016.12.FOCUS16430

Biswal, B., Yetkin, F. Z., Haughton, V. M., & Hyde, J. S. (1995). Functional connectivity in the motor cortex of resting human brain using echo-planar MRI. . *Magnetic resonance in medicine: official journal of the Society of Magnetic Resonancein Medicine / Society of Magnetic Resonance in Medicine., 34*(4), 537-541.

Corp, I. (Released 2015). IBM SPSS Statistics for Windows, Version 23.0. Armonk, NY

IBM Corp.

Cremers, H. R., Wager, T. D., & Yarkoni, T. (2017). The relation between statistical power and inference in fMRI. *PLoS One, 12*(11), e0184923. Retrieved from https://www.ncbi.nlm.nih.gov/pubmed/29155843. doi:10.1371/journal.pone.0184923

Cup, E. H., Ijspeert, J., Janssen, R. J., Bussemaker-Beumer, C., Jacobs, J., Pieterse, A. J., . . . van Alfen, N. (2013). Residual complaints after neuralgic amyotrophy. *Arch Phys Med Rehabil, 94*(1), 67-73. Retrieved from https://www.ncbi.nlm.nih.gov/pubmed/22850488. doi:10.1016/j.apmr.2012.07.014

Desikan, R. S., Segonne, F., Fischl, B., Quinn, B. T., Dickerson, B. C., Blacker, D., . . . Killiany, R. J. (2006). An automated labeling system for subdividing the human cerebral cortex on MRI scans into gyral based regions of interest. *Neuroimage, 31*(3), 968-980. Retrieved from https://www.ncbi.nlm.nih.gov/pubmed/16530430. doi:10.1016/j.neuroimage.2006.01.021

Di Vita, A., Boccia, M., Palermo, L., Nemmi, F., Traballesi, M., Brunelli, S., . . . Guariglia, C. (2018). Cerebellar grey matter modifications in lower limb amputees not using prosthesis. *Sci Rep, 8*(1), 370. Retrieved from https://www.ncbi.nlm.nih.gov/pubmed/29321625. doi:10.1038/s41598-017-18772-2

Douaud, G., Smith, S., Jenkinson, M., Behrens, T., Johansen-Berg, H., Vickers, J., . . . James, A. (2007). Anatomically related grey and white matter abnormalities in adolescent-onset schizophrenia. *Brain, 130*(Pt 9), 2375-2386. Retrieved from https://www.ncbi.nlm.nih.gov/pubmed/17698497. doi:10.1093/brain/awm184

Edwards, L. L., King, E. M., Buetefisch, C. M., & Borich, M. R. (2019). Putting the "Sensory" Into Sensorimotor Control: The Role of Sensorimotor Integration in Goal-Directed Hand Movements After Stroke. *Front Integr Neurosci, 13*, 16. Retrieved from https://www.ncbi.nlm.nih.gov/pubmed/31191265. doi:10.3389/fnint.2019.00016

Feng, J. T., Liu, H. Q., Hua, X. Y., Gu, Y. D., Xu, J. G., & Xu, W. D. (2016). Brain functional network abnormality extends beyond the sensorimotor network in brachial plexus injury patients. *Brain Imaging Behav, 10*(4), 1198-1205. Retrieved from https://www.ncbi.nlm.nih.gov/pubmed/26630882. doi:10.1007/s11682-015-9484-3

Good, C. D., Johnsrude, I. S., Ashburner, J., Henson, R. N., Friston, K. J., & Frackowiak, R. S. (2001). A voxel-based morphometric study of ageing in 465 normal adult human brains. *Neuroimage, 14*(1 Pt 1), 21-36. Retrieved from https://www.ncbi.nlm.nih.gov/pubmed/11525331. doi:10.1006/nimg.2001.0786

Gopinath, K., Krishnamurthy, V., Cabanban, R., & Crosson, B. A. (2015). Hubs of Anticorrelation in High-Resolution Resting-State Functional Connectivity Network Architecture. *Brain Connect, 5*(5), 267-275. Retrieved from https://www.ncbi.nlm.nih.gov/pubmed/25744222. doi:10.1089/brain.2014.0323

Greicius, M. D., Flores, B. H., Menon, V., Glover, G. H., Solvason, H. B., Kenna, H., . . . Schatzberg, A. F. (2007). Resting-state functional connectivity in major depression: abnormally increased contributions from subgenual cingulate cortex and thalamus. *Biological Psychiatry, 62*, 429-437.

Grieve, K. L., Acuna, C., & Cudeiro, J. (2000). The primate pulvinar nuclei: vision and action. *Trends in Neuroscience, 23*(1), 35-39.

Griffanti, L., Douaud, G., Bijsterbosch, J., Evangelisti, S., Alfaro-Almagro, F., Glasser, M. F., . . . Smith, S. M. (2017). Hand classification of fMRI ICA noise components. *Neuroimage, 154*, 188-205. Retrieved from https://www.ncbi.nlm.nih.gov/pubmed/27989777. doi:10.1016/j.neuroimage.2016.12.036

Gummesson, C., Atroshi, I., and Ekdahl, C. (2003). The disabilities of the arm, shoulder and hand (DASH) outcome questionnaire: longitudinal construct validity and measuring self-rated health change after surgery. *BMC Musculoskeletal Disorders, 4*(11), 1-6.

Gupta, R., & Tranel, D. (2012). Memory, Neural substrates. *Encyclopedia of Human Behavior (Seond Edition)*, 593-600.

Hara, Y. (2015). Brain plasticity and rehabilitation in stroke patients. *J Nippon Med Sch, 82*(1), 4-13. Retrieved from https://www.ncbi.nlm.nih.gov/pubmed/25797869. doi:10.1272/jnms.82.4

Helmich, R. C., de Lange, F. P., Bloem, B. R., & Toni, I. (2007). Cerebral compensation during motor imagery in Parkinson's disease. *Neuropsychologia, 45*(10), 2201-2215. Retrieved from https://www.ncbi.nlm.nih.gov/pubmed/17448507. doi:10.1016/j.neuropsychologia.2007.02.024

Hsu, C. L., Best, J. R., Voss, M. W., Handy, T. C., Beauchet, O., Lim, C., & Liu-Ambrose, T. (2019). Functional Neural Correlates of Slower Gait Among Older Adults With Mild Cognitive Impairment. *J Gerontol A Biol Sci Med Sci, 74*(4), 513-518. Retrieved from https://www.ncbi.nlm.nih.gov/pubmed/29471385. doi:10.1093/gerona/gly027

Ijspeert, J., Janssen, R. M., Murgia, A., Pisters, M. F., Cup, E. H., Groothuis, J. T., & van Alfen, N. (2013). Efficacy of a combined physical and occupational therapy intervention in patients with subacute neuralgic amyotrophy: a pilot study. *NeuroRehabilitation, 33*(4), 657-665. Retrieved from https://www.ncbi.nlm.nih.gov/pubmed/24004606. doi:10.3233/NRE-130993

Jang, S. H. (2013). Motor function-related maladaptive plasticity in stroke: a review. *NeuroRehabilitation, 32*(2), 311-316. Retrieved from https://www.ncbi.nlm.nih.gov/pubmed/23535793. doi:10.3233/NRE-130849

Jenkinson, M., Bannister, P., Brady, M., & Smith, S. (2002a). Improved Optimisation for the Robust and Accurate Linear Registration and Motion Correction of Brain Images. *Neuroimage, 2*(17), 825-841.

Jenkinson, M., Bannister, P., Brady, M., & Smith, S. (2002b). Improved Optimization for the Robust and Accurate Linear Registration and Motion Correction of Brain Images. *Neuroimage, 17*(2), 825-841. doi:10.1006/nimg.2002.1132

Jenkinson, M., Beckmann, C. F., Behrens, T. E., Woolrich, M. W., & Smith, S. M. (2012). Fsl. *Neuroimage, 62*(2), 782-790. Retrieved from https://www.ncbi.nlm.nih.gov/pubmed/21979382. doi:10.1016/j.neuroimage.2011.09.015

Lam, T. K., Dawson, D. R., Honjo, K., Ross, B., Binns, M. A., Stuss, D. T., . . . Chen, J. L. (2018). Neural coupling between contralesional motor and frontoparietal networks correlates with motor ability in individuals with chronic stroke. *J Neurol Sci, 384*, 21-29. Retrieved from https://www.ncbi.nlm.nih.gov/pubmed/29249372. doi:10.1016/j.jns.2017.11.007

Lee, M. H., Smyser, C. D., & Shimony, J. S. (2013). Resting-state fMRI: a review of methods and clinical applications. *AJNR Am J Neuroradiol, 34*(10), 1866-1872. Retrieved from https://www.ncbi.nlm.nih.gov/pubmed/22936095. doi:10.3174/ajnr.A3263

Li, W., Li, Y., Zhu, W., & Chen, X. (2014). Changes in brain functional network connectivity after stroke. *Neural Regen Res, 9*(1), 51-60. Retrieved from https://www.ncbi.nlm.nih.gov/pubmed/25206743. doi:10.4103/1673-5374.125330

Li, X. Y., Wan, Y., Tang, S. J., Guan, Y., Wei, F., & Ma, D. (2016). Maladaptive Plasticity and Neuropathic Pain. *Neural Plast, 2016*, 2. Retrieved from https://www.ncbi.nlm.nih.gov/pubmed/26925270. doi:10.1155/2016/4842159

Liu, B., Li, T., Tang, W. J., Zhang, J. H., Sun, H. P., Xu, W. D., . . . Feng, X. Y. (2013). Changes of inter-hemispheric functional connectivity between motor cortices after brachial plexuses injury: a resting-state fMRI study. *Neuroscience, 243*, 33-39. Retrieved from https://www.ncbi.nlm.nih.gov/pubmed/23562580. doi:10.1016/j.neuroscience.2013.03.048

Lou, L., Shou, T., Li, Z., Li, W., & Gu, Y. (2006). Transhemispheric functional reorganization of the motor cortex induced by the peripheral contralateral nerve transfer to the injured arm. *Neuroscience, 138*(4), 1225-1231. Retrieved from https://www.ncbi.nlm.nih.gov/pubmed/16426770. doi:10.1016/j.neuroscience.2005.11.062

Lu, Y., Liu, H., Hua, X., Xu, J. G., Gu, Y. D., & Shen, Y. (2016). Attenuation of brain grey matter volume in brachial plexus injury patients. *Neurol Sci, 37*(1), 51-56. Retrieved from https://www.ncbi.nlm.nih.gov/pubmed/26255300. doi:10.1007/s10072-015-2356-1

Lustenhouwer, R., Cameron, I. G. M., van Alfen, N., Oorsprong, T. D., Toni, I., van Engelen, B. G. M., . . . Helmich, R. C. (2020). Altered sensorimotor representations after recovery from peripheral nerve damage in neuralgic amyotrophy. *Cortex, 127*, 180-190. Retrieved from https://www.ncbi.nlm.nih.gov/pubmed/32203744. doi:10.1016/j.cortex.2020.02.011

Maeda, Y., Kettner, N., Holden, J., Lee, J., Kim, J., Cina, S., . . . Napadow, V. (2014). Functional deficits in carpal tunnel syndrome reflect reorganization of primary somatosensory cortex. *Brain, 137*(Pt 6), 1741-1752. Retrieved from https://www.ncbi.nlm.nih.gov/pubmed/24740988. doi:10.1093/brain/awu096

Murphy, K., Birn, R. M., Handwerker, D. A., Jones, T. B., & Bandettini, P. A. (2009). The impact of global signal regression on resting state correlations: are anti-correlated

networks introduced? *Neuroimage, 44*(3), 893-905. Retrieved from https://www.ncbi.nlm.nih.gov/pubmed/18976716. doi:10.1016/j.neuroimage.2008.09.036

Neitzer, A., Sun, S., Doss, S., Moran, J., & Schiller, B. (2012). Beck Depression Inventory-Fast Screen (BDI-FS): an efficient tool for depression screening in patients with end-stage renal disease. *Hemodial Int, 16*(2), 207-213. Retrieved from https://www.ncbi.nlm.nih.gov/pubmed/22754932. doi:10.1111/j.1542-4758.2012.00663.x

Nickerson, L. D., Smith, S. M., Ongur, D., & Beckmann, C. F. (2017). Using Dual Regression to Investigate Network Shape and Amplitude in Functional Connectivity Analyses. *Front Neurosci, 11*, 115. Retrieved from https://www.ncbi.nlm.nih.gov/pubmed/28348512. doi:10.3389/fnins.2017.00115

Oldfield, R. C. (1971). The Assessment and Analysis of Handedness: The Edinburgh Inventory. *Neuropsychologia, 9*, 97-113.

Paulraj, S. R., Schendel, K., Curran, B., Dronkers, N. F., & Baldo, J. V. (2018). Role of the left hemisphere in visuospatial working memory. *J Neurolinguistics, 48*, 133-141. Retrieved from https://www.ncbi.nlm.nih.gov/pubmed/31341351. doi:10.1016/j.jneuroling.2018.04.006

Peters, S. K., Dunlop, K., & Downar, J. (2016). Cortico-Striatal-Thalamic Loop Circuits of the Salience Network: A Central Pathway in Psychiatric Disease and Treatment. *Front Syst Neurosci, 10*, 104. Retrieved from https://www.ncbi.nlm.nih.gov/pubmed/28082874. doi:10.3389/fnsys.2016.00104

Poudel, G. R., Egan, G. F., Churchyard, A., Chua, P., Stout, J. C., & Georgiou-Karistianis, N. (2014). Abnormal synchrony of resting state networks in premanifest and symptomatic Huntington disease: the IMAGE-HD study. *J Psychiatry Neurosci, 39*(2), 87-96.

Retrieved from https://www.ncbi.nlm.nih.gov/pubmed/24083458. doi:10.1503/jpn.120226

Pruim, R. H. R., Mennes, M., van Rooij, D., Llera, A., Buitelaar, J. K., & Beckmann, C. F. (2015). ICA-AROMA: A robust ICA-based strategy for removing motion artifacts from fMRI data. *Neuroimage, 112*, 267-277. Retrieved from https://www.ncbi.nlm.nih.gov/pubmed/25770991. doi:10.1016/j.neuroimage.2015.02.064

Ramkiran, S., Sharma, A., & Rao, N. P. (2019). Resting-state anticorrelated networks in Schizophrenia. *Psychiatry Res Neuroimaging, 284*, 1-8. Retrieved from https://www.ncbi.nlm.nih.gov/pubmed/30605823. doi:10.1016/j.pscychresns.2018.12.013

Reddy, H., Bendahan, D., Lee, M. A., Johansen-Berg, H., Donaghy, M., Hilton-Jones, D., & Matthews, P. M. (2002). An expanded cortical representation for hand movement after peripheral motor denervation. *J Neurol Neurosurg Psychiatry*, *72*(2), 203-210. Retrieved from https://www.ncbi.nlm.nih.gov/pubmed/11796770. doi:10.1136/jnnp.72.2.203

Satterthwaite, T. D., Elliott, M. A., Gerraty, R. T., Ruparel, K., Loughead, J., Calkins, M. E., . . . Wolf, D. H. (2013). An improved framework for confound regression and filtering for control of motion artifact in the preprocessing of resting-state functional connectivity data. *Neuroimage, 64*, 240-256. Retrieved from https://www.ncbi.nlm.nih.gov/pubmed/22926292. doi:10.1016/j.neuroimage.2012.08.052

Schaefer, S. Y., Haaland, K. Y., & Sainburg, R. L. (2009). Hemispheric specialization and functional impact of ipsilesional deficits in movement coordination and accuracy. *Neuropsychologia, 47*(13), 2953-2966. Retrieved from

https://www.ncbi.nlm.nih.gov/pubmed/19573544. doi:10.1016/j.neuropsychologia.2009.06.025

Smith, A. T., Cotton, P. L., Bruno, A., & Moutsiana, C. (2009). Dissociating vision and visual attention in the human pulvinar. *J Neurophysiol, 101*(2), 917-925. Retrieved from https://www.ncbi.nlm.nih.gov/pubmed/19073806. doi:10.1152/jn.90963.2008

Smith, S. M. (2002). Fast robust automated brain extraction. *Hum Brain Mapp, 17*(3), 143-155. Retrieved from https://www.ncbi.nlm.nih.gov/pubmed/12391568. doi:10.1002/hbm.10062

Smith, S. M., Fox, P. T., Miller, K. L., Glahn, D. C., Fox, M., Mackay, C. E., . . . Beckmann, C. F. (2009). Correspondence of the brain's functional architecture during activation and rest. *Proceedings of the National Academy of Sciences, 106*(31), 13040-13045.

Smith, S. M., Jenkinson, M., Woolrich, M. W., Beckmann, C. F., Behrens, T. E., Johansen-Berg, H., . . . Matthews, P. M. (2004). Advances in functional and structural MR image analysis and implementation as FSL. *Neuroimage, 23 Suppl 1*, S208-219. Retrieved from https://www.ncbi.nlm.nih.gov/pubmed/15501092. doi:10.1016/j.neuroimage.2004.07.051

Solodkin, A., Hlustik, P., Chen, E. E., & Small, S. L. (2004). Fine modulation in network activation during motor execution and motor imagery. *Cereb Cortex, 14*(11), 1246-1255. Retrieved from https://www.ncbi.nlm.nih.gov/pubmed/15166100. doi:10.1093/cercor/bhh086

Staines, W. R., Padilla, M. P., & Knight, R. T. (2002). Frontal-parietal event-related potential changes associated with practising a novel visuomotor task. *Cognitive Brain Research, 13*, 195-202.

Travor, I., Parker Jones, O., Mars, R. B., Smith, S. M., Behrens, T. E., & Jbabdi, S. (2016). Task-free MRI predicts individual differences in brain activity during task performance. *Science, 352*(6282), 216-220.

Tyll, S., Budinger, E., & Noesselt, T. (2011). Thalamic influences on multisensory integration. *Commun Integr Biol, 4*(4), 378-381. Retrieved from https://www.ncbi.nlm.nih.gov/pubmed/21966551. doi:10.4161/cib.4.4.15222

Van Eijk, J. J., Groothuis, J. T., & Van Alfen, N. (2016). Neuralgic amyotrophy: An update on diagnosis, pathophysiology, and treatment. *Muscle Nerve, 53*(3), 337-350. Retrieved from https://www.ncbi.nlm.nih.gov/pubmed/26662794. doi:10.1002/mus.25008

van Nuenen, B. F., Helmich, R. C., Buenen, N., van de Warrenburg, B. P., Bloem, B. R., & Toni, I. (2012). Compensatory activity in the extrastriate body area of Parkinson's disease patients. *J Neurosci, 32*(28), 9546-9553. Retrieved from https://www.ncbi.nlm.nih.gov/pubmed/22787040. doi:10.1523/JNEUROSCI.0335-12.2012

WHO. (2001). International classification of functioning, disability, and health: ICF. *Geneva: World Health Organization*.

Winkler, A. M., Ridgway, G. R., Webster, M. A., Smith, S. M., & Nichols, T. E. (2014). Permutation inference for the general linear model. *Neuroimage, 92*, 381-397. Retrieved from https://www.ncbi.nlm.nih.gov/pubmed/24530839. doi:10.1016/j.neuroimage.2014.01.060

Zeller, D., & Classen, J. (2014). Plasticity of the motor system in multiple sclerosis. *Neuroscience, 283*, 222-230. Retrieved from https://www.ncbi.nlm.nih.gov/pubmed/24881573. doi:10.1016/j.neuroscience.2014.05.043

Zhang, Y., Brady, M., & Smith, S. (2001). Segmentation of Brain MR Images Through a Hidden Markov Random Field Model and the Expectation-Maximization Alogrithm. *IEEE Transactions of Medical Imaging, 20*(1), 45-57.